



# CHALMERS

## Chalmers Publication Library

### **A Stochastic Geometry Model for Vehicular Communication near Intersections**

This document has been downloaded from Chalmers Publication Library (CPL). It is the author's version of a work that was accepted for publication in:

**IEEE Globecom Workshops**

Citation for the published paper:

Steinmetz, E. ; Wildemeersch, M. ; Quek, T. et al. (2015) "A Stochastic Geometry Model for Vehicular Communication near Intersections". IEEE Globecom Workshops

Downloaded from: <http://publications.lib.chalmers.se/publication/228394>

Notice: Changes introduced as a result of publishing processes such as copy-editing and formatting may not be reflected in this document. For a definitive version of this work, please refer to the published source. Please note that access to the published version might require a subscription.

Chalmers Publication Library (CPL) offers the possibility of retrieving research publications produced at Chalmers University of Technology. It covers all types of publications: articles, dissertations, licentiate theses, masters theses, conference papers, reports etc. Since 2006 it is the official tool for Chalmers official publication statistics. To ensure that Chalmers research results are disseminated as widely as possible, an Open Access Policy has been adopted. The CPL service is administrated and maintained by Chalmers Library.

(article starts on next page)

# A Stochastic Geometry Model for Vehicular Communication near Intersections

Erik Steinmetz<sup>\*†</sup>, Matthias Wildemeersch<sup>‡</sup>, Tony Q.S. Quek<sup>‡</sup>, and Henk Wymeersch<sup>\*</sup>

<sup>\*</sup>Department of Signals and Systems, Chalmers University of Technology, Gothenburg, Sweden

<sup>†</sup>SP Technical Research Institute of Sweden, Borås, Sweden

<sup>‡</sup>Singapore University of Technology and Design, Singapore

email: estein@chalmers.se

**Abstract**—Many traffic-related applications require the nodes in a vehicular ad-hoc network (VANET) to periodically broadcast their state information. As measurements campaigns or simulations to evaluate the reliability of packet transmission are slow and scenario-specific, we present an analytic performance assessment tool that accounts for the spatial statistics of the nodes on a road, in a scenario of crossing roads and fast fading. Based on stochastic geometry, our tool is able to capture a static two-dimensional road geometry and the effect of interference due to node clustering in the vicinity of an intersection. Numerical results reveal how packet transmission is affected as the receiver gets closer to the intersection.

## I. INTRODUCTION

Vehicular ad-hoc networks (VANETs) are regarded as one of the key enablers in future intelligent transportation systems (ITS) [1]–[6], and are envisioned to pave the way for a new set of applications that will enhance both traffic safety and efficiency. In addition, VANETs will create a huge potential for infotainment services that offer convenience and comfort to the driver [1], [2].

To meet the communication demand of future ITS applications spectrum has been allocated in the 5.9 GHz band, and the IEEE 802.11p standard has been defined, allowing for vehicle-to-vehicle (V2V) and vehicle-to-infrastructure (V2I) communication in 10 and 20 MHz channels. However, different applications clearly have different requirements on the communication links, and the most stringent demands are imposed by safety-related applications. To increase the time to react in critical situations and to obtain full situational awareness these require relatively long communication ranges, extremely low latencies (below 50 ms in pre-crash situations), as well as high delivery ratios [7], [8]. These requirements in combination with a possible high density of vehicles, constant topology changes as well as rapidly changing signal propagation conditions makes the design of VANET communication challenging.

Extensive simulations and measurement campaigns are often used to guide the design process [7], [9]. However, these are often scenario-specific and time consuming, creating a need for analytical expressions of key-performance metrics that can be used to gain quick insights about scalability and performance. In particular for two important scenarios: highways and intersections. Stochastic geometry is a tool to

obtain such expressions, and has been widely used in the design and analysis of wireless networks [10]. Previous work focusing on VANETs, and that includes the spatial statistics of vehicles, typically considers a one-dimensional linear road [11]–[15]. However, effects due to intersections have been briefly studied in [16], [17], indicating that it is important to properly model interference from different roads and the clustering of vehicles close to the intersection. Clustering has been addressed by considering Poisson cluster processes [18] and Cox processes [13], leading to complex models.

In this paper, we extend the work in [16] and present an analytical model for the reception probability, tailored to intersection scenarios. Our model is based on stochastic geometry and characterizes the packet reception probability in a VANET as a function of the distance between the receiver and the transmitter, accounting for the increased interference a car will experience in the vicinity of an intersection, and realistic signal propagation models. The main contribution of this work is to capture the clustering of vehicles in the vicinity of an intersection by means of a relatively simple and tractable model. This model can be used to gain insights when designing vehicular communications systems, and as a complement to simulations and measurements to understand the effect of interference in VANETs.

## II. SYSTEM MODEL

We consider an intersection scenario with two perpendicular single-lane roads, as shown in Fig. 1. The two roads are indicated by  $X$  and  $Y$ , and each carries cars according to a one-dimensional homogeneous Poisson point process (PPP). The intensities of cars on the two roads are  $\lambda_X$  and  $\lambda_Y$ , such that the two point processes describing the locations of the cars on the two roads are represented by  $\Phi_X \sim \text{PPP}(\lambda_X)$  and  $\Phi_Y \sim \text{PPP}(\lambda_Y)$ . The positions of individual vehicles (also referred to as nodes) on the two roads  $X$  and  $Y$  are denoted by  $\mathbf{x}_i = [x_i, 0]^T$  and  $\mathbf{y}_i = [0, y_i]^T$ , respectively.

As both V2V and V2I communication are of interest we consider a transmitter with arbitrary location (marked as a red dot in Fig. 1). The transmitter broadcasts its state information with a fixed transmission power  $P$ . We consider a receiver on road  $X$  at location  $\mathbf{x}_{\text{rx}} = [x_{\text{rx}}, 0]^T$  (marked with a green dot in Fig. 1) at a distance  $d = |x_{\text{rx}}|$  from the intersection.

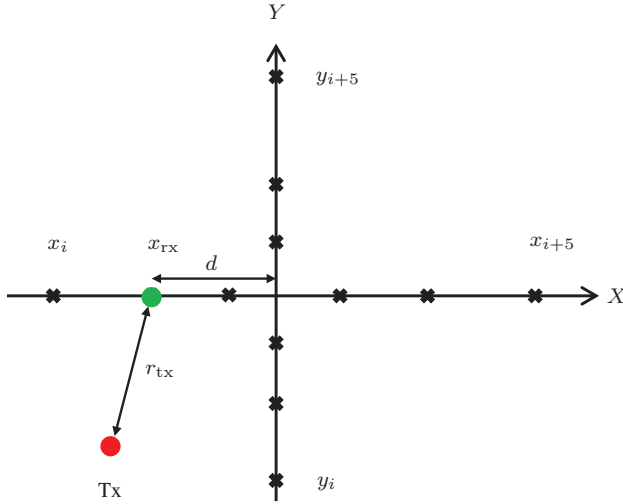


Figure 1. System model consisting of two perpendicular single-lane roads. The transmitter of interest is marked in red and can be at any location, while the target receiver which is marked in green is located on road  $X$ . Vehicles on road  $X$  and  $Y$  are represented by crosses, a fraction  $p$  of which transmits concurrently and causes interference.

The signal propagation modeled comprises Rayleigh multipath fading with exponential power fading  $h$ , and path loss  $l(r_{\text{tx}}) = (Ar_{\text{tx}})^{-\alpha}$ , where  $r_{\text{tx}}$  is the distance between the transmitter and the receiver,  $\alpha$  is the path loss exponent, and  $A$  is a constant that depends on antenna characteristics. Shadowing effects are neglected. At the receiver, the signal is further affected by white Gaussian noise with variance  $\sigma^2$  and interference from other transmitting vehicles. At any time, the fraction of transmitting vehicles that contributes to the aggregate interference is denoted by  $p \in [0, 1]$ , leading to PPPs  $\Phi_X^1$  and  $\Phi_Y^1$  with intensities  $p\lambda_X$  and  $p\lambda_Y$ , respectively. Note that the transmitter Tx does not necessarily belong to  $\Phi_X^1$  and  $\Phi_Y^1$ .

Our aim is to analytically characterize the probability that the receiver  $x_{\text{rx}}$  successfully receives a packet sent by the transmitter, accounting for the clustering effect with decreased distance  $d$  to the intersection. Successful reception occurs when the signal-to-interference-plus-noise ratio (SINR) exceeds a threshold  $\zeta$ .

### III. PACKET RECEPTION PROBABILITY

#### A. General expression

The probability that the receiver  $x_{\text{rx}}$  successfully decodes a transmission from the transmitter can be expressed as

$$\mathbb{P}_s(\zeta) = \Pr[\text{SINR} > \zeta] \quad (1)$$

$$= \Pr\left[\frac{Phl(r_{\text{tx}})}{I_X + I_Y + \sigma^2} > \zeta\right], \quad (2)$$

where  $I_X$  (resp.  $I_Y$ ) is the aggregate interference originating from active nodes on road  $X$  (resp. road  $Y$ ), which is given

by

$$I_X = \sum_{x \in \Phi_X^1} Ph_x l(\|\mathbf{x}_{\text{rx}} - \mathbf{x}\|) \quad (3)$$

$$I_Y = \sum_{y \in \Phi_Y^1} Ph_y l(\|\mathbf{x}_{\text{rx}} - \mathbf{y}\|), \quad (4)$$

in which  $\mathbf{x} = [x, 0]^T$  and  $\mathbf{y} = [0, y]^T$ . The receiver  $x_{\text{rx}}$  can be any of the non-transmitting cars on road<sup>1</sup>  $X$ , while the transmitter can be located anywhere.<sup>2</sup>

We can rewrite the success probability as

$$\mathbb{P}_s(\zeta) = \mathbb{E}_{I_X, I_Y} \left[ \Pr\left(h > \frac{\zeta}{Pl(r_{\text{tx}})}(I_X + I_Y + \sigma^2)\right) \right]. \quad (5)$$

Due to the Rayleigh fading, where the power  $h \sim \exp(1)$ , we get

$$\begin{aligned} \mathbb{P}_s(\zeta) &= \exp\left(\frac{-\zeta(Ar_{\text{tx}})^\alpha \sigma^2}{P}\right) \\ &\times \mathbb{E}_{I_X, I_Y} \left[ \exp\left(\frac{-\zeta(Ar_{\text{tx}})^\alpha I_X}{P}\right) \exp\left(\frac{-\zeta(Ar_{\text{tx}})^\alpha I_Y}{P}\right) \right], \end{aligned} \quad (6)$$

and using the independence of the PPPs on roads  $X$  and  $Y$ , we finally have that

$$\begin{aligned} \mathbb{P}_s(\zeta) &= \\ \mathcal{L}_{I_X} \left( \frac{\zeta(Ar_{\text{tx}})^\alpha}{P} \right) \mathcal{L}_{I_Y} \left( \frac{\zeta(Ar_{\text{tx}})^\alpha}{P} \right) \exp\left(\frac{-\zeta(Ar_{\text{tx}})^\alpha \sigma^2}{P}\right), \end{aligned} \quad (7)$$

where  $\mathcal{L}(\cdot)$  stands for the Laplace transform. The three factors in (7) can be interpreted as follows: the first factor is the reduction of the success probability due to the interference from the own road; the second factor is the reduction of the success probability due to the interference from the perpendicular road; and the third factor is the success probability in the interference free case. Note that  $\mathcal{L}_{I_Y}(\zeta(Ar_{\text{tx}})^\alpha/P)$  depends on the distance to the intersection  $d$ .<sup>3</sup>

We are now ready to determine expressions for both  $\mathcal{L}_{I_X}(\zeta(Ar_{\text{tx}})^\alpha/P)$  and  $\mathcal{L}_{I_Y}(\zeta(Ar_{\text{tx}})^\alpha/P)$  in the sections below.

#### B. Effect of interference from own road

Considering a one-dimensional PPP, the Laplace transform of the aggregate interference originating from the own road is

<sup>1</sup>In case the receiver does not belong to either road  $X$  or  $Y$ , a slight modification to the analysis is required.

<sup>2</sup>Note that in case Tx belongs to  $\Phi_X$  or  $\Phi_Y$ , the results still hold due to Slivnyak's Theorem [10, Theorem A.5].

<sup>3</sup>We have ignored the speed distribution on both roads and the clustering induced by the reduced speed in the vicinity of the intersection.

given by

$$\mathcal{L}_{I_X}(s) = \mathbb{E}[\exp(-sI_X)] \quad (8)$$

$$= \mathbb{E} \left[ \prod_{x \in \Phi_X} \exp(-sPh_x(A|x_{\text{rx}} - x|)^{-\alpha}) \right] \quad (9)$$

$$\stackrel{(a)}{=} \mathbb{E}_{\Phi_X} \left[ \prod_{x \in \Phi_X} \mathbb{E}_{h_x} \{ \exp(-sPh_x(A|x_{\text{rx}} - x|)^{-\alpha}) \} \right] \quad (10)$$

$$= \mathbb{E}_{\Phi_X} \left[ \prod_{x \in \Phi_X} \frac{1}{1 + sP(A|x_{\text{rx}} - x|)^{-\alpha}} \right] \quad (11)$$

$$\stackrel{(b)}{=} \exp \left( -p\lambda_X \int_{-\infty}^{+\infty} \frac{1}{1 + (A|x_{\text{rx}} - x|)^{\alpha}/sP} dx \right) \quad (12)$$

$$\stackrel{(c)}{=} \exp \left( -p\lambda_X (sP)^{1/\alpha} \frac{2}{A} \int_0^{+\infty} \frac{1}{1 + u^\alpha} du \right) \quad (13)$$

$$= \exp \left( -p\lambda_X (sP)^{1/\alpha} \frac{2}{A} \pi/\alpha \csc(\pi/\alpha) \right) \quad (14)$$

where (a) holds due to the independence of the fading parameters, (b) uses the expression of the probability generating functional (PGFL) for a PPP [10, Definition A.5], and (c) involves a change of variable  $A|x_{\text{rx}} - x|/(sP)^{1/\alpha} \rightarrow u$ . Substituting  $s = \zeta(Ar_{\text{tx}})^\alpha/P$  yields the desired result:

$$\mathcal{L}_{I_X} \left( \frac{\zeta(Ar_{\text{tx}})^\alpha}{P} \right) = \exp \left( -2p\lambda_X \zeta^{1/\alpha} r_{\text{tx}} \pi/\alpha \csc(\pi/\alpha) \right). \quad (15)$$

For the particular cases of  $\alpha \in \{2, 4\}$ , this further simplifies to

$$\mathcal{L}_{I_X} \left( \frac{\zeta(Ar_{\text{tx}})^2}{P} \right) = \exp \left( -p\lambda_X \sqrt{\zeta} r_{\text{tx}} \pi \right) \quad (16)$$

$$\mathcal{L}_{I_X} \left( \frac{\zeta(Ar_{\text{tx}})^4}{P} \right) = \exp \left( -p\lambda_X \zeta^{1/4} r_{\text{tx}} \pi/\sqrt{2} \right). \quad (17)$$

### C. Effect of interference from perpendicular road

For the second factor in (7), we can apply the same expectation over the fading and interferers' positions, leading to<sup>4</sup>

$$\mathcal{L}_{I_Y}(s) = \exp \left( - \int_{-\infty}^{+\infty} \frac{p\lambda_Y}{1 + (A \|\mathbf{x}_{\text{rx}} - \mathbf{y}\|)^\alpha / sP} dy \right). \quad (21)$$

<sup>4</sup>Alternatively, the two-dimensional scenario can be reduced to a single road scenario by the projection of every point of  $\Phi_Y$  on the X-axis, resulting in the PPP  $\Phi_{X'} = f(\Phi_Y)$ , with  $f: \mathbb{R}^2 \rightarrow \mathbb{R}^2$  defined by  $\mathbf{x}'_i = f(\mathbf{y}_i) = [\sqrt{y_i^2 + d^2}, 0]^\top$ . According to the mapping theorem [10, Theorem A.1], the Poisson law is preserved under the mapping  $f$ , such that  $\Phi_{X'}$  is a (non-homogeneous) PPP. The non-homogeneous density of the transformed PPP can be found using

$$\int_{\mathcal{A}} \lambda_Y(\mathbf{y}) d\mathbf{y} = \int_{f(\mathcal{A})} \lambda_Y(f^{-1}(x)) \left| \frac{\partial f^{-1}(x)}{\partial x} \right| dx, \quad (18)$$

where  $\mathcal{A}$  is the domain of integration. We find that the intensity of the transformed PPP is given by

$$\lambda_{X'}(x) = \lambda_Y(f^{-1}(x)) \left| \frac{\partial f^{-1}(x)}{\partial x} \right|. \quad (19)$$

Note that  $\|\mathbf{x}_{\text{rx}} - \mathbf{y}\| = \sqrt{x_{\text{rx}}^2 + y^2} = \sqrt{d^2 + y^2}$ . We introduce  $r_y = \sqrt{d^2 + y^2}$ , with  $dr_y/dy = y/r_y$ . This leads to

$$\mathcal{L}_{I_Y}(s) = \exp \left( -2p\lambda_Y \int_d^{+\infty} \frac{r_y}{\sqrt{r_y^2 - d^2} (1 + (Ar_y)^\alpha / sP)} dr_y \right) \quad (22)$$

$$= \exp \left( -p\lambda_Y \frac{(sP)^{1/\alpha}}{A} \int_{\omega_0}^{+\infty} \frac{1}{\sqrt{\omega - \omega_0} (1 + \omega^{\alpha/2})} d\omega \right), \quad (23)$$

where we have carried out the following change of variable  $(Ar_y/((sP)^{1/\alpha}))^2 \rightarrow \omega$ , and further introduced  $\omega_0 = (Ad/((sP)^{1/\alpha}))^2$ . The integral can be computed in closed-form for  $\alpha = 2$  and  $\alpha = 4$ , with

$$\int_{\omega_0}^{+\infty} \frac{1}{\sqrt{\omega - \omega_0} (1 + \omega)} d\omega = \frac{\pi}{\sqrt{1 + \omega_0}} \quad (24)$$

$$\int_{\omega_0}^{+\infty} \frac{1}{\sqrt{\omega - \omega_0} (1 + \omega^2)} d\omega = \frac{\pi \sin \left( \frac{1}{2} \arctan \frac{1}{\omega_0} \right)}{(1 + \omega_0^2)^{1/4}}. \quad (25)$$

Evaluating (23) for  $s = \zeta(Ar_{\text{tx}})^\alpha/P$  and  $\alpha \in \{2, 4\}$ , finally yields

$$\mathcal{L}_{I_Y} \left( \frac{\zeta(Ar_{\text{tx}})^2}{P} \right) = \exp \left( - \frac{p\lambda_Y \pi r_{\text{tx}}^2 \zeta}{\sqrt{d^2 + r_{\text{tx}}^2 \zeta}} \right) \quad (26)$$

and

$$\mathcal{L}_{I_Y} \left( \frac{\zeta(Ar_{\text{tx}})^4}{P} \right) = \exp \left( - \frac{p\lambda_Y \pi r_{\text{tx}}^2 \sqrt{\zeta} \sin \left( \frac{1}{2} \arctan \left( \frac{r_{\text{tx}}^2 \sqrt{\zeta}}{d^2} \right) \right)}{(d^4 + r_{\text{tx}}^4 \zeta)^{1/4}} \right). \quad (27)$$

Note that for  $d \rightarrow 0$ , (26)–(27) revert to (16)–(17), while for  $d \rightarrow +\infty$ , both (26) and (27) tend to one.

## IV. EXTENSIONS

The model developed above can easily be extended to more complex scenarios. Here, we briefly describe two extensions.

### A. Extension to multi-lane scenarios

The independence of the PPPs enables us to factorize the success probability into separate factors for the interference contribution from each lane. We can add additional lanes at any distance from the receiver with any orientation. For

Considering  $f(\mathbf{y}) = [\sqrt{y^2 + d^2}, 0]^\top$  and  $\Phi_Y$  homogeneous with constant density  $\lambda_Y$ , we find that

$$\lambda_{X'}(x) = \frac{\lambda_Y x}{\sqrt{x^2 - d^2}}. \quad (20)$$

Using this density function in (12) and mapping the domain of integration, we find (22). Although less intuitive, this method provides insight how the density of a one-dimensional PPP on a line changes for an observation point at a distance  $d$  from the line. Moreover, this method lends itself better to cover more involved scenarios with different road geometries and non-homogeneous node densities.

example, for the four-lane scenario shown in Fig. 2 and  $\alpha = 2$ , the success probability can be expressed as

$$\begin{aligned} \mathbb{P}_s(\zeta) = & \quad (28) \\ & \underbrace{\exp\left(-p\lambda_{X_1}\sqrt{\zeta}r_{\text{tx}}\pi\right)}_{\text{own road}} \underbrace{\exp\left(-\frac{p\lambda_{X_2}\pi r_{\text{tx}}^2\zeta}{\sqrt{d_{\text{road}}^2+r_{\text{tx}}^2\zeta}}\right)}_{\text{parallel road}} \\ & \times \underbrace{\exp\left(-\frac{p\lambda_{Y_1}\pi r_{\text{tx}}^2\zeta}{\sqrt{d^2+r_{\text{tx}}^2\zeta}}\right)}_{\text{far perpendicular road}} \underbrace{\exp\left(-\frac{p\lambda_{Y_2}\pi r_{\text{tx}}^2\zeta}{\sqrt{(d-d_{\text{road}})^2+r_{\text{tx}}^2\zeta}}\right)}_{\text{near perpendicular road}} \\ & \times \exp\left(\frac{-\zeta(Ar_{\text{tx}})^\alpha\sigma^2}{P}\right). \end{aligned}$$

### B. Extension to non-homogeneous PPPs

As pointed out in [13], a homogeneous PPP may not be realistic as it does not capture reduced vehicle speed near the intersection, and more sophisticated models may be required. In such a case, (21) can be generalized by allowing  $\lambda_Y$  to be a function of  $y$ , i.e.,  $\lambda_Y(y)$ . Following the same change of variables, and assuming the intensity to be symmetric around the intersection, we find that

$$\begin{aligned} \mathcal{L}_{I_Y}(s) = & \quad (29) \\ & \exp\left(-p\frac{(sP)^{1/\alpha}}{A}\int_{\omega_0}^{+\infty}\frac{\lambda_Y(d\sqrt{\omega/\omega_0-1})}{\sqrt{(\omega-\omega_0)(1+\omega^{\alpha/2})}}d\omega\right). \end{aligned}$$

Depending on the functional  $\lambda_Y(d\sqrt{\omega/\omega_0-1})$ , the integral in (29) can be evaluated in closed form. As an example, for  $\alpha = 2$  and  $\lambda_Y(y)$  linearly decaying from  $\lambda_h$  at the intersection to a value  $\lambda_l \leq \lambda_h$  at a distance  $\Delta > 0$  away from the intersection, according to

$$\lambda_Y(y) = \begin{cases} -(\lambda_h - \lambda_l)|y|/\Delta + \lambda_h & |y| < \Delta \\ \lambda_l & |y| \geq \Delta, \end{cases} \quad (30)$$

it can be shown that

$$\begin{aligned} \mathcal{L}_{I_Y}\left(\zeta\frac{(Ar_{\text{tx}})^2}{P}\right) = & \quad (31) \\ & \exp\left(-\frac{pr_{\text{tx}}^2\zeta\lambda_l\pi}{\sqrt{d^2+r_{\text{tx}}^2\zeta}}\right) \\ & \times \exp\left(\frac{(\lambda_h - \lambda_l)pr_{\text{tx}}^2\zeta}{\Delta}\log\left(1 + \frac{\Delta^2}{d^2+r_{\text{tx}}^2\zeta}\right)\right) \\ & \times \exp\left(-\frac{2(\lambda_h - \lambda_l)pr_{\text{tx}}^2\zeta}{\sqrt{d^2+r_{\text{tx}}^2\zeta}}\arctan\left(\frac{\Delta}{\sqrt{d^2+r_{\text{tx}}^2\zeta}}\right)\right). \end{aligned}$$

For the own road, a symmetric PPP around the intersection does not lead to a symmetric PPP with respect to the receiver position. Hence, the integrals, which will now depend on the relative position of the receiver with respect to the PPP intensity profile, will be much more involved. For an intensity of the form (30) along road  $X$ , we see that  $\lambda_X(x) = \lambda_l + \lambda_X(x) - \lambda_l$ ,

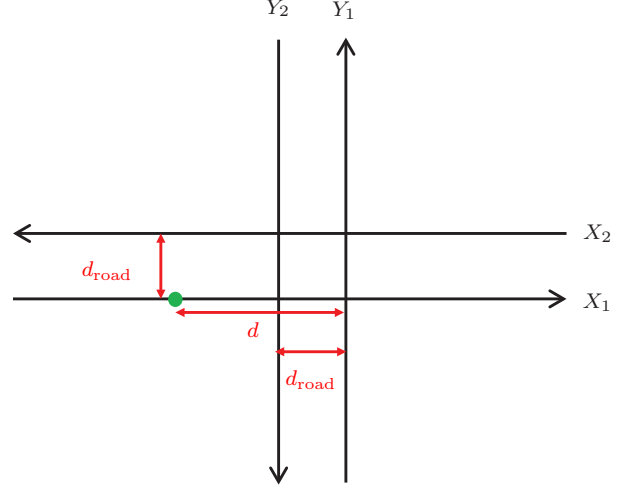


Figure 2. Scenario with multiple lanes. Parallel roads are separated by a fixed distance  $d_{\text{road}}$ .

in which  $\lambda_X(x) - \lambda_l$  is nonzero only for  $|x| < \Delta$ . Hence,

$$\begin{aligned} \mathcal{L}_{I_X}(s) = & \quad (32) \\ & \exp\left(-\int_{-\infty}^{+\infty}\frac{p\lambda_l}{1+(A|x_{\text{rx}}-x|)^\alpha/sP}dx\right) \\ & \times \exp\left(-\int_{-\Delta}^{\Delta}\frac{p(\lambda_X(x)-\lambda_l)}{1+(A|x_{\text{rx}}-x|)^\alpha/sP}dx\right), \end{aligned}$$

in which the first factor is of the form (12). The value of the second factor depends on  $d$  and on whether or not  $x_{\text{rx}}$  is in the interval  $[-\Delta, +\Delta]$ . Under general assumptions for the intensity function, the success probability can be found by numerically solving a single integral. However, when  $\lambda_X(x)$  is piecewise linear, closed-form expressions can be found for all integrals for all values of  $\alpha$  (for  $\alpha = 2$ , these specialize to involve  $\arctan(\cdot)$  and  $\log(\cdot)$ , similar to (31)).

## V. NUMERICAL RESULTS

### A. Scenario

We consider a scenario with two orthogonal roads with equal intensity  $\lambda_X = \lambda_Y = 0.01$  (i.e., with an average inter-vehicle distance of 100 m). We assume a noise variance  $\sigma^2$  of  $-99$  dBm, a path-loss exponent  $\alpha = 2$ , and an SINR threshold of  $\zeta = 8$  dB [9]. Furthermore, we assume that  $A = 650$ , and we set the transmit power to  $P = 100$  mW (i.e., 20 dBm). For visualization purposes, we will show the outage probability  $\mathbb{P}_{\text{out}}(\zeta) = 1 - \mathbb{P}_s(\zeta)$ .

### B. Results and discussion

Fig. 3 shows the outage probability  $\mathbb{P}_{\text{out}}(\zeta)$  as a function of the distance  $r_{\text{tx}}$  between the receiver and the transmitter, for three different transmit probabilities  $p \in \{0, 0.01, 0.1\}$  and three different distances to the intersection  $d \in \{0, 100 \text{ m}, 500 \text{ m}\}$ . In the absence of interferers ( $p = 0$ ), the system achieves an outage of 10% at a distance of  $r_{\text{tx}} \approx$

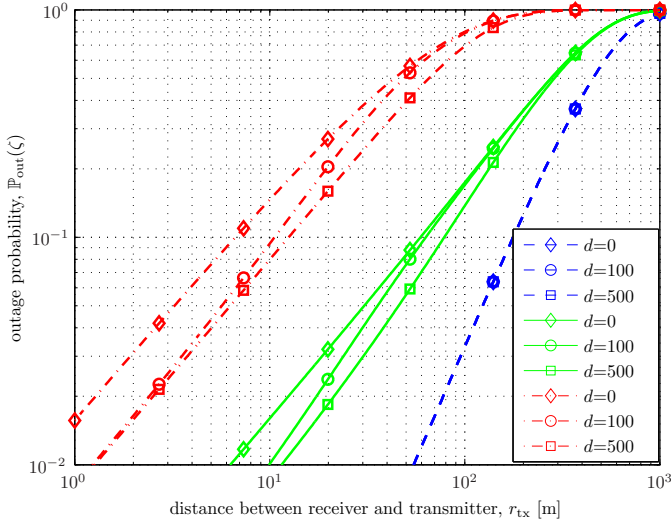


Figure 3. Outage probability  $\mathbb{P}_{\text{out}}(\zeta)$  as a function of  $r_{\text{tx}}$  for three different transmit probabilities  $p = 0$  (blue),  $p = 0.01$  (green), and  $p = 0.1$  (red), and different distances to the intersection  $d \in \{0, 100 \text{ m}, 500 \text{ m}\}$ .

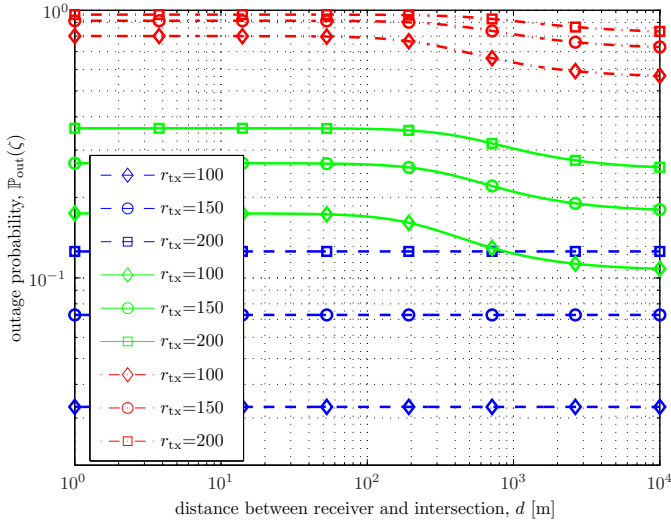


Figure 4. Outage probability  $\mathbb{P}_{\text{out}}(\zeta)$  as a function of  $d$  for three different transmit probabilities  $p = 0$  (blue),  $p = 0.01$  (green) and  $p = 0.1$  (red), and different distances between transmitter and receiver  $r_{\text{tx}} \in \{100 \text{ m}, 150 \text{ m}, 200 \text{ m}\}$ .

200 m. When  $p$  is increased to 0.01, the communication range is reduced to around 60 m at the same outage. Higher outages are observed when the receiver is closer to the intersection. The communication range is further reduced to around 10 m when  $p = 0.1$ . Interestingly, for low outage probabilities, the performance seems insensitive to the distance to intersection  $d > 0$ .

To more clearly see the effect of the distance  $d$  to the intersection, Fig. 4 shows the outage probability  $\mathbb{P}_{\text{out}}(\zeta)$  as a function of  $d$  for the three transmit probabilities  $p \in \{0, 0.01, 0.1\}$ . For  $p = 0$ , the value of  $d$  plays no role, while for  $p = 0.01$  and  $p = 0.1$ , the  $\mathbb{P}_{\text{out}}(\zeta)$  is more or less constant as a function of  $d$ , for  $d \in [0, 100 \text{ m}]$ , so that the interference level is more or less

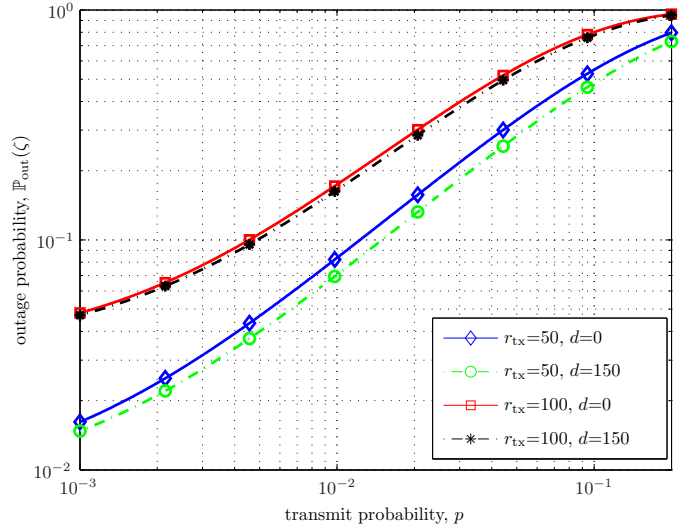


Figure 5. Outage probability  $\mathbb{P}_{\text{out}}(\zeta)$  as a function of the transmit probability  $p$  for four different combinations of  $r_{\text{tx}} \in \{50 \text{ m}, 100 \text{ m}\}$  and  $d \in \{0 \text{ m}, 150 \text{ m}\}$ .

independent of the distance to the intersection. For  $d > 100 \text{ m}$ , the outage probability decreases and for  $d > 1 \text{ km}$ ,  $\mathbb{P}_{\text{out}}(\zeta)$  settles down to a value where the perpendicular road no longer contributes with noticeable interference.

Fig. 5 shows the outage probability  $\mathbb{P}_{\text{out}}(\zeta)$  as a function of the transmit probability  $p$ , for four different combinations of  $d$  and  $r_{\text{tx}}$ . As before, we observe that the outage probability increases when the transmit probability increases. Moreover, we can see that a change in the distance  $r_{\text{tx}}$  between the receiver and transmitter has a larger impact on the outage probability than a change in the distance  $d$  between the receiver and the intersection.

For the sake of completeness, we have extended the results from Fig. 3 to a scenario with four lanes (as shown in Fig. 2), with equal intensities of vehicles on all lanes ( $\lambda = 0.01$ ), and a distance  $d_{\text{road}} = 5 \text{ m}$ . In Fig. 6 numerical values on the outage probability are shown for the four-lane case for transmit probabilities  $p \in \{0, 0.01, 0.1\}$ . Comparing the four-lane scenario with the results from the two-lane scenario, we can see that we have a slightly decreased transmission range (for the same outage probability) due to the fact that more interfering nodes are present.

## VI. CONCLUSIONS

In this paper, we have presented a model based on stochastic geometry to evaluate the reliability of packet transmissions in VANETs in the vicinity of intersections. We have characterized the packet reception probability as a function of the distance between the receiver and the transmitter, accounting for relevant network parameters such as the spatial distribution of the nodes on the roads, the increased interference due to clustering of users close to the intersection, and the properties of the wireless propagation channel. We provide closed form expressions on the packet reception probability, for several

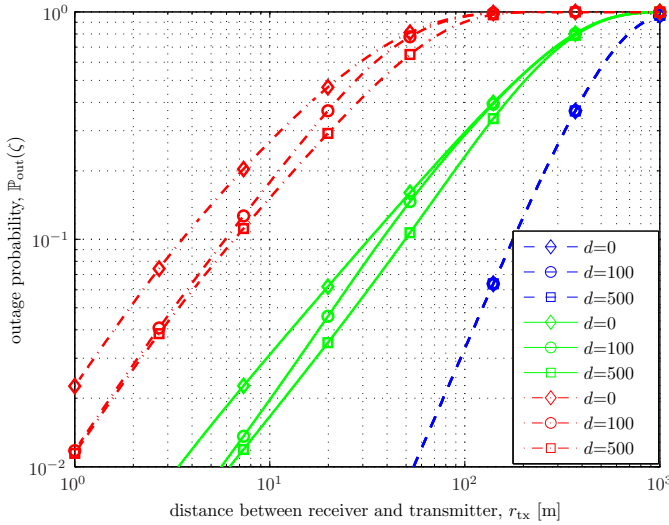


Figure 6. Outage probability for the four lane scenario as a function of  $r_{tx}$  for three different transmit probabilities  $p = 0$  (blue),  $p = 0.01$  (green) and  $p = 0.1$  (red), and different distances to the intersection  $d \in \{0, 100 \text{ m}, 500 \text{ m}\}$ .

cases of practical relevance. Furthermore, we have demonstrated how the model can be extended to an arbitrary number of lanes with different orientations and to account for increased vehicle density near the intersection.

The proposed model can be used to gain insights when designing vehicular communication systems, and as a complement to simulations or measurements. It can also be useful when designing control algorithms that should be robust to communication impairments.

Future work includes the adoption of realistic medium access control (MAC), the inclusion of shadowing due to obstacles (e.g., buildings and large vehicles), and the validation against existing numerical models.

#### ACKNOWLEDGMENTS

This research was supported in part, by the European Research Council, under Grant No. 258418 (COOPNET), the EU project HIGHTS (High precision positioning for cooperative ITS applications) MG- 3.5a-2014-636537, and VINNOVA, under the program “Nationell Metrologi vid SP Sveriges Tekniska Forskningsinstitut.”

#### REFERENCES

[1] G. Karagiannis, O. Altintas, E. Ekici, G. Heijnen, B. Jarupan, K. Lin, and T. Weil, “Vehicular Networking: A Survey and Tutorial on Requirements, Architectures, Challenges, Standards and Solutions,” *IEEE Communications Surveys & Tutorials*, vol. 13, no. 4, pp. 584–616, 2011.

[2] P. Papadimitratos, A. La Fortelle, K. Evensen, R. Brignolo, and S. Cosenza, “Vehicular Communication Systems: Enabling Technologies, Applications, and Future Outlook on Intelligent Transportation,” *IEEE Communications Magazine*, vol. 47, pp. 84–95, Nov. 2009.

[3] H. Hartenstein and K. Laberteaux, “A Tutorial Survey on Vehicular Ad Hoc Networks,” *IEEE Communications Magazine*, vol. 46, pp. 164–171, June 2008.

[4] K. Dar, M. Bakhouya, J. Gaber, M. Wack, and P. Lorenz, “Wireless Communication Technologies for ITS Applications [Topics in Automotive Networking],” *IEEE Communications Magazine*, vol. 48, pp. 156–162, May 2010.

[5] F. Anjum, S. Choi, V. Gligor, R. Herrtwich, J.-P. Hubaux, P. Kumar, R. Shorey, and C.-T. Lea, “Guest Editorial Vehicular Networks,” *IEEE Journal on Selected Areas in Communications*, vol. 25, pp. 1497–1500, Oct. 2007.

[6] M. Alsabaan, W. Alasmay, A. Albasir, and K. Naik, “Vehicular Networks for a Greener Environment: A Survey,” *IEEE Communications Surveys & Tutorials*, vol. 15, pp. 1372–1388, Jan. 2013.

[7] C. F. Mecklenbrauker, A. F. Molisch, J. Karedal, F. Tufvesson, A. Paier, L. Bernado, T. Zemen, O. Klemp, and N. Czink, “Vehicular Channel Characterization and Its Implications for Wireless System Design and Performance,” *Proceedings of the IEEE*, vol. 99, pp. 1189–1212, July 2011.

[8] J. Santa, R. Toledo-Moreo, M. A. Zamora-Izquierdo, B. Úbeda, and A. F. Gómez-Skarmeta, “An analysis of communication and navigation issues in collision avoidance support systems,” *Transportation Research Part C: Emerging Technologies*, vol. 18, pp. 351–366, June 2010.

[9] K. Sjöberg, *Medium Access Control for Vehicular Ad Hoc Networks*. PhD thesis, Chalmers University of Technology, 2013.

[10] M. Haenggi and R. K. Ganti, “Interference in Large Wireless Networks,” *Foundations and Trends in Networking*, vol. 3, no. 2, pp. 127–248, 2008.

[11] B. Błaszczyszyn, P. Mühlthaler, and Y. Toor, “Stochastic analysis of Aloha in vehicular ad hoc networks,” *Annales des télécommunications - Annales des télécommunications*, vol. 68, pp. 95–106, June 2012.

[12] B. Błaszczyszyn, P. Mühlthaler, and N. Achir, “Vehicular Ad-hoc Networks using slotted Aloha: Point-to-Point, Emergency and Broadcast Communications,” in *2012 IFIP Wireless Days*, pp. 1–6, IEEE, Nov. 2012.

[13] Y. Jeong, J. W. Chong, H. Shin, and M. Z. Win, “Intervehicle Communication: Cox-Fox Modeling,” *IEEE Journal on Selected Areas in Communications*, vol. 31, pp. 418–433, Sept. 2013.

[14] B. Błaszczyszyn, P. Mühlthaler, and Y. Toor, “Performance of MAC protocols in linear VANETs under different attenuation and fading conditions,” in *IEEE Conference on Intelligent Transportation Systems, Proceedings, ITSC*, pp. 715–720, IEEE, Oct. 2009.

[15] Z. Tong, H. Lu, M. Haenggi, and C. Poellabauer, “A Stochastic Geometry Approach to the Modeling of IEEE 802.11p for Vehicular Ad Hoc Networks,” *Submitted to IEEE Transactions on Vehicular Technology*, 2015.

[16] E. Steinmetz, M. Wildemeersch, and H. Wymeersch, “WiP abstract: Reception probability model for vehicular ad-hoc networks in the vicinity of intersections,” in *2014 ACM/IEEE International Conference on Cyber-Physical Systems (ICCPS)*, vol. 68, pp. 223–223, IEEE, Apr. 2014.

[17] E. Steinmetz, R. Hult, G. R. de Campos, M. Wildemeersch, P. Falcone, and H. Wymeersch, “Communication analysis for centralized intersection crossing coordination,” in *International Symposium on Wireless Communications Systems (ISWCS)*, pp. 813–818, 2014.

[18] R. K. Ganti and M. Haenggi, “Interference and Outage in Clustered Wireless Ad Hoc Networks,” *IEEE Transactions on Information Theory*, vol. 55, pp. 4067–4086, Sept. 2009.